Am J Transl Res 2019;11(5):3092-3100
www.ajtr.org /ISSN:1943-8141/AJTR0089111

Original Article

New experimental animal model of intracardiac thrombus created with epicardial echocardiographic guidance

Yang Wang[1], David H Hsi[3], Weiming Yuan[2], Jingru Lin[1], Zhenghui Zhu[1], Kunjing Pang[1], Hao Wang[1], Weichun Wu[1]

Departments of [1]Echocardiography, [2]Cardiac Experiment Surgery, Fuwai Hospital, National Center for Cardiovascular Diseases, Beijing, China; [3]Department of Cardiology, Stamford Hospital, Stamford, CT, USA

Received November 28, 2018; Accepted April 1, 2019; Epub May 15, 2019; Published May 30, 2019

Abstract: Background: Models of intracardiac thrombus are very difficult to establish and have rarely been reported. We designed and established a new, inexpensive, practical animal model for intracardiac thrombus created with epicardial echocardiographic guidance. Methods: Male New Zealand white rabbits weighing 2 to 3.9 kg (3.10±0.58 kg) were used in this study. Cylindrical thrombi were created in plastic tubing and then aspirated with saline into a syringe. The thrombus in saline suspension was then slowly injected into a heart chamber and confirmed with echocardiography, including two-dimensional and contrast-enhanced ultrasound. Results: Intracardiac thrombi were created successfully in the left ventricle, right ventricle, and left and right atrial appendages. The average preparation time was about 3 hours. There were no significant differences among the four heart chambers in the success rate of thrombus model creation. Thrombi embolized to the pulmonary artery after failure of the right heart model. After failure of the left heart model, emboli were found in the carotid artery, renal artery, and truncus coeliacus. In two cases thrombi extended from the left ventricular apex into the aorta and in one case the thrombus extended from the left atrial appendage to the left atrium; there was no such extension from the other chambers. The rabbits' vital signs remained stable after establishment of the model, with no significant changes in heart structure or function. Conclusions: This new method of creating an intracardiac thrombus model in rabbits showed initial success.

Keywords: Thrombosis model, ultrasound examination, blood coagulation, vital signs

Introduction

Thromboembolic diseases, such as acute myocardial infarction, ischemic cerebrovascular disease, and pulmonary embolism, are important causes of death. Ultrasound imaging has the advantages of being inexpensive and noninvasive without radiation while providing real-time imaging with high spatial resolution. The currently available study models are generally for vascular thrombosis [1-3]. Models of intracardiac thrombus are very difficult to establish and very rarely reported [4]. We designed and established a new, inexpensive, practical animal model of cardiac thrombus created with epicardial echocardiographic guidance.

Methods

The study protocol was approved by the institutional Experimental Animal Center and Echocardiography Department, National Center for Cardiovascular Diseases, Fuwai Hospital, China and the National Animal Ethics Committee.

Eight male New Zealand white rabbits weighing 2 to 3.9 kg (3.10±0.58 kg) were used in this study. A thrombus was injected into each of the four heart chambers in each rabbit, in the following order: left atrium, left ventricle, right atrium, and right ventricle (1). We drew 2 to 3 ml of blood from the rabbit's ear vein with a disposable intravenous infusion needle and stored the sample in long plastic tubing at room temperature for about 3 hours for thrombus formation (diameter 0.4 cm, length approximately 20 cm). After 3 hours, we put the prepared thrombus into a container filled with saline, then aspirated the thrombus with saline into a 2-ml syringe (**Figure 1A-C**) (2). The animals were anesthetized with sodium pentobarbital (30 mg/kg) and mechanically ventilated. We obtained ba-

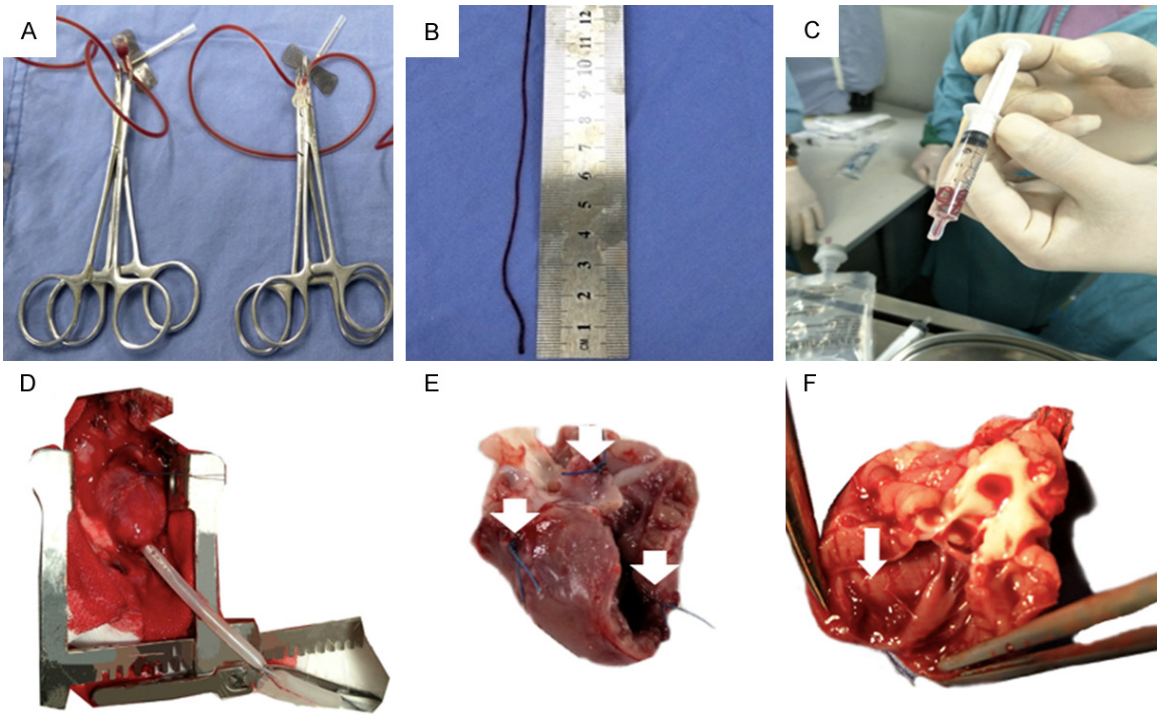

Figure 1. A. Blood samples were kept in plastic tubing for 3 hours at room temperature. B. Thrombi can be created in different lengths. The blood clot shown in the figure measures 0.4×12 cm. C. Blood clot in saline suspension. D. A 20-g trocar is passed through the heart wall within the purse-string suture. E. Positions of purse-string sutures (white arrows). F. Left ventricular apical clot (white arrows).

seline two-dimensional ultrasound and color Doppler images in apical and parasternal views (Vivid E9; GE, Milwaukee, WI; 2D mode and S12 probe) (**Figure 2D**, **2E**) (3). The rabbits were placed in the supine position and a midline incision was made to expose the pericardium. We placed purse-string sutures with 4×12 silk at the injection sites, including left ventricular apex, atrial appendages (atrial thrombi), and right ventricular wall/right ventricular outflow tract (right ventricular thrombus). A 20-g trocar was used to penetrate the heart wall within the purse-string suture (**Figure 1D**). After confirming with epicardial ultrasound that the needle was located in the ventricular or atrial cavity, the syringe containing the thrombus and saline was attached to the cannula. Echocardiography was used to monitor as the thrombus in saline suspension was slowly pushed into the heart chamber (**Figure 2**). The rabbit hearts were inspected postmortem to verify the location of thrombi. The extracardiac large vessels (pulmonary artery, aortic arch and its branches, thoracic aorta, abdominal aorta, celiac trunk, renal artery, and common iliac artery and its branches) were also explored to determine the embolic location of detached thrombi.

Results

All intracardiac thrombus models were created successfully. Thrombi were created in the left ventricle (**Figure 2A**, **2D**), right ventricle (**Figure 2B**, **2E**), and left and right atrial appendages (**Figure 2C**, **2F**). The average preparation time was about 3 hours. Thrombus length was generally 10 to 20 cm. The length of the thrombus injected into the heart chamber can be controlled.

The left atrial model succeeded seven times and failed once. Postmortem examination revealed that the detached thromboembolism was located in the main trunk of the right renal artery. The left ventricular model succeeded five times and failed three times. Postmortem examination revealed detached thrombi in the right carotid artery (**Figure 3B**), truncus coeliacus, and left renal artery (**Figure 3A**). The right atrium model succeeded seven times and failed once. Postmortem examination revealed that the detached thrombus was located in the pulmonary artery (**Figure 3C**). The right ventricular model succeeded six times and failed twice. Postmortem examination revealed that both detached thrombi were located in the pulmo-

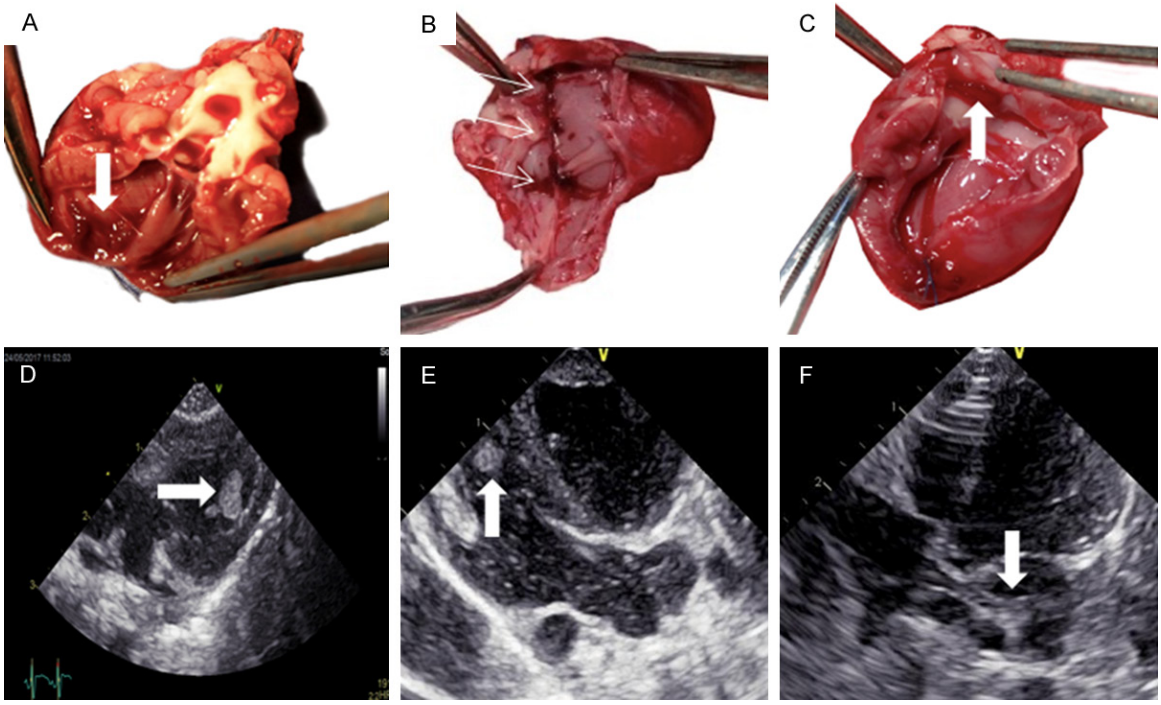

Figure 2. A-C. Cardiac specimens showing thrombi in the left ventricle, right ventricle, and left atrium (extension from left atrial appendage). D-F. Corresponding echocardiographic images showing thrombi (white arrows).

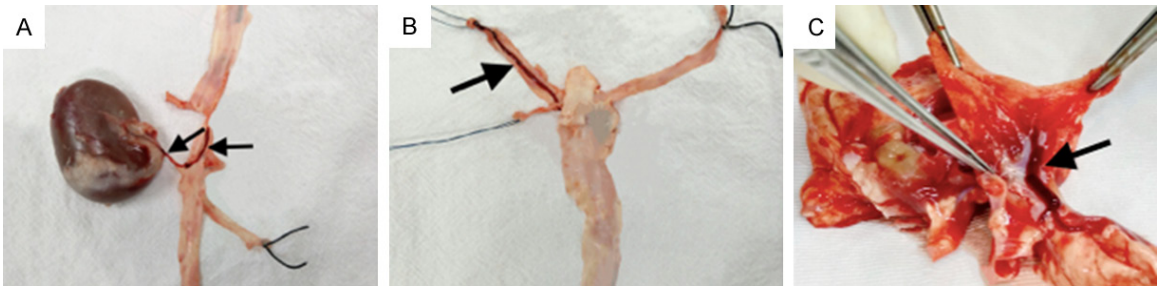

Figure 3. A. Thromboembolism in abdominal aorta and right renal artery. B. Thromboembolism in right carotid artery. C. Thromboembolism in pulmonary artery (black arrows).

Table 1. Success of thrombosis model creation in four heart chambers

	Success Times	Failure Times	Total	Success rate (%)
LA thrombosis model	7	1	8	87.5
LV thrombosis model	5	3	8	62.5
RA thrombosis model	7	1	8	87.5
RV thrombosis model	6	2	8	75.0
Total	25	7	32	78.1

This table shows the success rate of thrombus model creation in each of the four heart chambers (n=8 for each chamber). The success rates in the left atrium and right atrium were 87.5%, the success rate in the left ventricle was 62.5%, and the success rate in the right ventricle was 75.0%. The overall success rate of the heart chamber model was 78.1%. LA, left atrium; LV, left ventricle; RA, right atrium; RV, right ventricle.

nary artery (**Figure 3C**). The success rates of thrombosis model establishment in the left atrium, left ventricle, right atrium, and right ventricle were 87.5%, 62.5%, 87.5%, and 75.0%, respectively (**Table 1**).

SPSS 23.0 statistical software was used for analysis. Because half of the expected values in the experimental data were less than 5 (half of expected values were between 1 and 5), the Pearson chi-square test condition was not satisfied and only Fisher's exact test was used. There were no significant differences in the success rates of the four cardiac chamber models (P>0.05) (**Tables 1** and **2**).

Table 2. Fisher's exact test analysis of success rates of thrombosis models in the four heart chambers

	LA (n=8)	LV (n=8)	RA (n=8)	RV (n=8)	*P*-Value
Success Times	7 (78.5%)	5 (62.5%)	7 (78.5%)	6 (75.0%)	>0.05

The success rates of left atrial, left ventricular, right atrial, and right ventricular thrombosis models were 78.5%, 62.5%, 78.5%, and 75.0%, respectively. Fisher's exact test results for the four heart-chamber success rates show P>0.05. LA, left atrium; LV, left ventricle; RA, right atrium; RV, right ventricle.

Table 3. Characteristics of left atrial thrombosis model in rabbits

Variables	Before Model Making (n=8)	After Model Making (n=8)	*P* Value
Mean weight ± SD, kg	3.10±0.58	3.10±0.58	-
Mean body temperature ± SD, °C	36.85±0.55	36.68±0.56	0.16
Mean heart rate ± SD, bpm	213.65±22.04	205.50±16.72	0.10
Mean systolic blood pressure ± SD, mm Hg	86.25±7.23	85.00±5.98	0.51
Mean diastolic blood pressure ± SD, mm Hg	75.5±5.15	72.88±5.59	0.08

Values are presented as means ± SD.

Table 4. Characteristics of left ventricular thrombosis model in rabbits

Variables	Before Model Making (n=8)	After Model Making (n=8)	*P* Value
Mean weight ± SD, kg	3.10±0.58	3.10±0.58	-
Mean body temperature ± SD, °C	36.56±0.49	36.59±0.41	0.86
Mean heart rate ± SD, bpm	203.88±21.80	198.63±17.60	0.63
Mean systolic blood pressure ± SD, mm Hg	83.75±6.94	82.38±7.11	0.49
Mean diastolic blood pressure ± SD, mm Hg	71.50±3.82	68.50±5.58	0.06

Values are presented as means ± SD.

Table 5. Characteristics of right atrial thrombosis model in rabbits

Variables	Before Model Making (n=8)	After Model Making (n=8)	*P* Value
Mean weight ± SD, kg	3.10±0.58	3.10±0.58	-
Mean body temperature ± SD, °C	36.51±0.53	36.40±0.39	0.39
Mean heart rate ± SD, bpm	199.63±16.16	188.88±28.04	0.37
Mean systolic blood pressure ± SD, mm Hg	80.00±7.98	79.38±9.08	0.85
Mean diastolic blood pressure ± SD, mm Hg	66.50±5.10	65.50±8.09	0.73

Values are presented as means ± SD.

In two cases the thrombus extended from the left ventricular apex into the aorta and in one case it extended from the left atrial appendage into the left ventricle. In addition, right atrial thrombus crosses the tricuspid valve, causing tricuspid insufficiency.

All eight rabbits survived after the model was established. The rabbits' heart structure and function did not change after modeling (**Tables 3-6**). The vital signs of five rabbits remained stable, with body temperature, heart rate, systolic blood pressure, and diastolic blood pressure in the normal range (**Tables 7-10**). In the remaining three rabbits, heart rate, systolic blood pressure, and diastolic blood pressure decreased significantly after thrombus detachment from the right heart but returned to normal after 30 minutes (**Tables 7-10**).

Discussion

We created in an in vivo rabbit model by inserting emboli directly into the heart. Thrombi formed at room temperature in approximately 3 hours and were usually composed of stable red thrombus [5]. In this study, we tried different clotting times ranging from 1 to 4 hours and

Table 6. Characteristics of right ventricular thrombosis model in rabbits

Variables	Before Model Making (n=8)	After Model Making (n=8)	*P* Value
Mean weight ± SD, kg	3.10±0.58	3.10±0.58	-
Mean body temperature ± SD, °C	36.58±0.49	36.51±0.38	0.58
Mean heart rate ± SD, bpm	195.50±16.58	171.63±30.17	0.12
Mean systolic blood pressure ± SD, mm Hg	82.63±3.54	76.50±10.97	0.13
Mean diastolic blood pressure ± SD, mm Hg	70.13±3.76	65.00±10.86	0.25

Values are presented as means ± SD.

Table 7. Cardiac structure and function in left atrial thrombosis model

	Before Model Making (n=8)	After Model Making (n=8)	*P* Value
Left atrium anterior-posterior diameter, cm	0.74±0.04	0.73±0.04	0.63
Right atrium left-right diameter, cm	0.81±0.05	0.81±0.05	0.76
Right ventricular anterior-posterior diameter, cm	0.62±0.01	0.61±0.01	0.08
Left ventricular end diastolic diameter, cm	1.38±0.02	1.37±0.02	0.17
Left ventricular end systolic volume, ml	1.46±0.11	1.43±0.09	0.33
Left ventricular end diastolic volume, ml	5±0	5±0	-
Ejection fraction, %	70.88±2.03	71.50±1.77	0.33

Values are presented as means ± SD.

Table 8. Cardiac structure and function in left ventricular thrombosis model

	Before Model Making (n=8)	After Model Making (n=8)	*P* Value
Left atrium anterior-posterior diameter, cm	0.74±0.03	0.75±0.03	0.30
Right atrium left-right diameter, cm	0.81±0.04	0.82±0.04	0.07
Right ventricular anterior-posterior diameter, cm	0.62±0.01	0.61±0.01	0.86
Left ventricular end diastolic diameter, cm	1.38±0.03	1.38±0.03	0.52
Left ventricular end systolic volume, ml	1.43±0.09	1.36±0.09	0.16
Left ventricular end diastolic volume, ml	5±0	5±0	...
Ejection fraction, %	71.38±1.85	71.75±1.58	0.65

Values are presented as means ± SD.

Table 9. Cardiac structure and function in right atrial thrombosis model

	Before Model Making (n=8)	After Model Making (n=8)	*P* Value
Left atrium anterior-posterior diameter, cm	0.75±0.03	0.75±0.03	1
Right atrium left-right diameter, cm	0.82±0.04	0.82±0.04	0.45
Right ventricular anterior-posterior diameter, cm	0.62±0.01	0.62±0.01	1
Left ventricular end diastolic diameter, cm	1.38±0.02	1.38±0.02	0.35
Left ventricular end systolic volume, ml	1.42±0.12	1.41±0.08	0.84
Left ventricular end diastolic volume, ml	5±0	5±0	-
Ejection fraction, %	71.63±2.33	71.75±1.58	0.84

Values are presented as means ± SD.

found that a 3-hour duration was most suitable for creating a stable thrombus. We explored different heart chambers for thrombus insertion. Statistical analysis revealed no differences among the four heart chambers in success rates of establishing thrombosis models. Before and after modeling, we used ultrasound to measure many parameters of heart size and function, including left atrium anterior-posterior diameter, right atrium left-right diameter, right ventricular anterior-posterior diameter, left ventricular end-diastolic diameter, left ventricular end-systolic volume, left ventricular end-diastolic volume, and left ventricular ejection fraction. Statistical analysis showed no significant changes in these values; heart structure and

Table 10. Cardiac structure and function in right ventricular thrombosis model

	Before Model Making (n=8)	After Model Making (n=8)	*P* Value
Left atrium anterior-posterior diameter, cm	0.73±0.04	0.73±0.04	1
Right atrium left-right diameter, cm	0.82±0.04	0.82±0.04	0.20
Right ventricular anterior-posterior diameter, cm	0.61±0.01	0.62±0.01	0.32
Left ventricular end diastolic diameter, cm	1.37±0.02	1.37±0.02	1
Left ventricular end systolic volume, ml	1.42±0.08	1.38±0.08	0.21
Left ventricular end diastolic volume, ml	5±0	5±0	-
Ejection fraction, %	71.63±1.69	72.50±1.60	0.21

Values are presented as means ± SD.

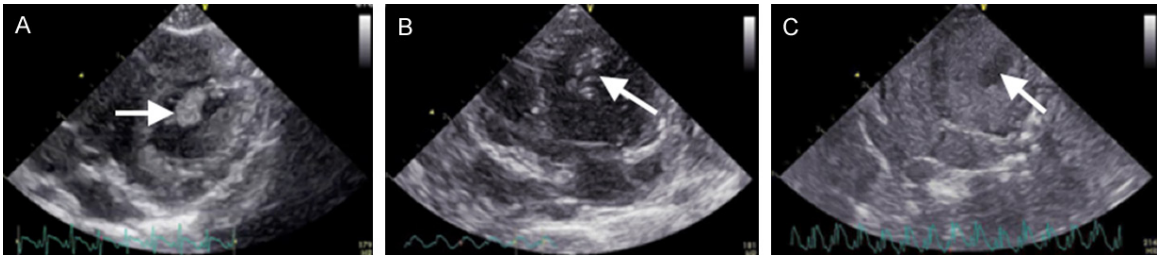

Figure 4. A. Ultrasonography: left ventricular short-axis view shows ovoid left ventricular thrombosis (white arrow). B. Ultrasonography: apical four-chamber view of left ventricular thrombus (white arrow). C. Contrast-enhanced ultrasonography: the left ventricular thrombus in the apical four-chamber view shows a low-anechoic filling defect; the high echo of the contrast microbubbles clearly outlines the thrombus (white arrow).

function were in the normal range both before and after modeling. We found that rabbits' vital signs, including body temperature, heart rate, systolic blood pressure, and diastolic blood pressure, remained normal after systemic embolism caused by thrombus shed from the left heart. However, thrombi shed from the right heart went directly into the pulmonary artery, causing pulmonary embolism. The heart rate and systolic and diastolic blood pressure of these rabbits decreased significantly and their vital signs showed transient instability but returned to normal after 30 minutes. Therefore, we conclude that the risk of making a thrombus model in the right heart is greater than that in the left heart. Through observation, we found that the left ventricular apex and right ventricular outflow tract were relatively easy locations for thrombus adhesion. We observed that the thrombi changed shape in the heart chamber and usually curled into a spherical form (**Figures 4A**, **4B**, **5B**). Sometimes the left ventricular thrombi extended to the aorta because of the high-pressure environment, causing aortic valve insufficiency. Thrombi also sometimes moved as a cylinder in the heart cavity, resulting in insufficiency of the corresponding valve (**Figure 5D-F**).

Hamilton and colleagues proposed a method for preparing left ventricular thrombus by ligating the apical coronary arteries of mixed-breed dogs and then injecting fibrin adhesive through the apical myocardium [4]. Although that method is feasible, the operation is complex, requiring not only initial creation of a myocardial infarction model, but also multistep laboratory preparation to inject the fibrin adhesive into the left ventricle. The final thrombosis differs from the common clinical fresh blood thrombus because of the effect of the fibrin core.

It is well known that the high energy produced during radiofrequency ablation can damage endothelial cells and produce ventricular or atrial thrombus [6]. Studies have shown that the greater the area of radiofrequency ablation, the higher the incidence of thrombus formation. The area, depth, and volume of lesions positively correlate with the volume of thrombus. We can use this method to make intracardiac thrombus, but the resulting thrombus size is not easy to control and embolic events are common.

Cardiac thrombosis is related to low-flow heart conditions; cardiac arrest is the ultimate low

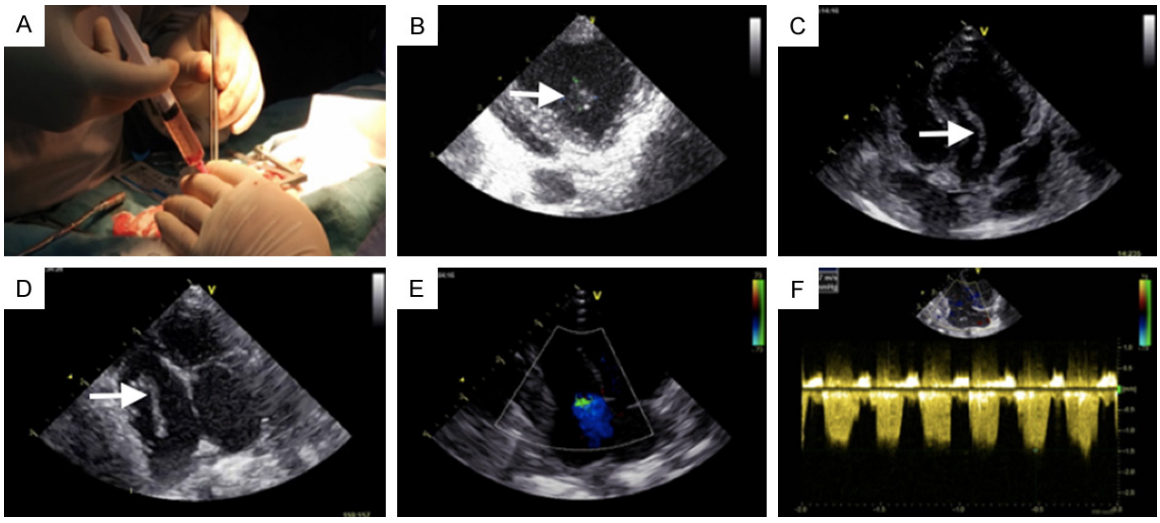

Figure 5. A. Thrombus injection into the heart cavity. This process is the key step in creating a successful thrombus model. The key is to master the strength and speed of injection to prevent loss of the thrombus. B. Left ventricular thrombus, curled into a spherical shape and measuring 0.4×0.5 cm. C. Left ventricular thrombus, extending across mitral valve. D. Right atrial thrombus, extending across tricuspid valve. E. Right atrial thrombus crosses the tricuspid valve, causing tricuspid insufficiency. Color Doppler: tricuspid regurgitation signal. F. Spectrum Doppler: the tricuspid regurgitation spectrum is shown.

blood flow state. Therefore, left ventricular thrombus can be formed with a cardiac arrest model [7]. In this method, ventricular fibrillation is induced to stop blood flow. Once blood flow stops, thrombus can appear within 6 minutes. This method has a high success rate; however, the acute thrombus formed will dissolve within a few minutes of early defibrillation or external chest compression. In addition, the method involves myocardial dysfunction, which results in blood stasis and thrombosis; restoration of function may lead to embolism.

Lian and colleagues used granulocyte colony-stimulating factor (G-CSF) to induce hypercoagulability. They created left ventricular thrombus in mice through the interaction of inflammation and thrombus [8]. That method creates left ventricular thrombosis approximately 4 weeks after intraperitoneal injection of G-CSF. Thus, the time needed to establish the model is relatively long.

We established a simple, feasible, and rapid modeling method in rabbits. Our thrombus model has potential applications. The diagnosis of intracardiac thrombus remains clinically important, with associated risks of systemic embolization and implications for antithrombotic management. In the future, we can use this model to evaluate different ultrasound contrast agents or targeted microbubbles approved for left ventricular opacification and endocardial border definition. Studies have demonstrated that targeted theranostic microbubbles can selectively bind to thrombi, allowing successful molecular ultrasound imaging of thrombosis [9]. However, the potential for bleeding may limit its broader use. A newly created innovative therapy combines echo-enhancing microbubbles and a fibrinolytic drug in the form of an activated-platelet-specific single-chain antibody [10]. Some studies have described the unique concept of a noninvasive, inexpensive, and widely available technology that can simultaneously detect thrombi, resolve vessel occlusion, and monitor success or failure of thrombolysis [11]. Additionally, we can study the mechanism of thrombolysis and strategies for decreasing the use of thrombolytics to avoid complications [12]. Furthermore, contrast-enhancing echocardiography can provide further assessment of the tissue characteristics of left ventricular masses suspicious for intracardiac thrombi. Differentiation of avascular thrombi from tumors will result in improved diagnostic performance of echocardiography [13].

This model can be applied to creating many related models, such as a pulmonary embolism model. We can deliberately detach the throm-

bus from the right heart to create a pulmonary embolism model. Similarly, models of systemic arterial embolism, such as renal artery thrombosis, can be created by deliberately detaching the thrombus from the left heart.

Conclusion

We explored a new method of creating an intracardiac thrombus model in rabbits, with initial success. This new animal model may help clinicians study the imaging characteristics of intracardiac thrombi of different clot sizes, attachment positions, and clotting times, as well as thrombus migration to the cerebral and peripheral circulation. Newly emerging thrombus-targeted contrast agents can specifically bind to and penetrate deep within thrombi, offering great potential in the detection of thrombotic diseases and the identification of many other diseases. A series of ultrasound thrombolysis studies could be performed on the basis of this thrombus model. We also hope to evaluate the safety and feasibility of ultrasound-facilitated thrombolysis within the heart in the early stage of clot formation. In addition, it is difficult to identify thrombus in some areas with conventional ultrasound. This model can also be used to create thrombi in these areas, allowing subsequent studies on thrombus detection methods (three-dimensional ultrasound imaging technology, contrast-enhanced ultrasound technology, etc.). This method of creating an intracardiac thrombus model is simple and stable. It provides an ideal new way to improve diagnostic technology and explore therapies for cardiac thrombosis. The establishment of this model has extensive popularization potential.

Acknowledgements

This work was supported by the PUMC Youth Fund (3332016013). We thank Rebecca Tollefson, DVM, from Liwen Bianji, Edanz Editing China (www.liwenbianji.cn/ac), for editing the English text of a draft of this manuscript.

Disclosure of conflict of interest

None.

Address correspondence to: Drs. Weichun Wu and Hao Wang, Department of Echocardiography, Fuwai Hospital, National Center for Cardiovascular Diseases, Chinese Academy of Medical Sciences and Peking Union Medical College, 167 Beilishi Road, Xicheng District, Beijing 100037, China. E-mail: achundoctor@163.com (WCW); hal6112@163.com (HW)

References

[1] Ma J, Li X, Wang Y, Yang Z, Luo J. Rivaroxaban attenuates thrombosis by targeting the NF-κB signaling pathway in a rat model of deep venous thrombus. Int J Mol Med 2017; 40: 1869-1880.

[2] Tang Z, Wang X, Huang J, Zhou X, Xie H, Zhu Q, Huang M, Ni S. Gene expression profiling of pulmonary artery in a rabbit model of pulmonary thromboembolism. PLoS One 2016; 31: e0164530.

[3] Yun X, Chen Y, Yang K, Wang S, Lu W, Wang J. Upregulation of canonical transient receptor potential channel in the pulmonary arterial smooth muscle of a chronic thromboembolic pulmonary hypertension rat model. Hypertens Res 2015; 38: 821-828.

[4] Hamilton A, Huang SL, Warnick D, Stein A, Rabbat M, Madhav T, Kane B, Nagaraj A, Klegerman M, MacDonald R, McPherson D. Left ventricular thrombus enhancement after intravenous injection of echogenic immunoliposomes: studies in a new experimental model. Circulation 2002; 11: 2772-2778.

[5] Zhang H, Cui YC, Tian Y, Yuan WM, Yang JZ, Peng P, Li K, Liu XP, Zhang D, Wu AL, Zhou Z, Tang Y. A novel model for evaluating thrombolytic therapy in dogs with ST-elevation myocardial infarction. BMC Cardiovasc Disord 2016; 25: 16-21.

[6] Khairy P, Chauvet P, Lehmann J, Lambert J, Macle L, Tanguay JF, Sirois MG, Santoianni D, Dubuc M. Lower incidence of thrombus formation with cryoenergy versus radiofrequency catheter ablation. Circulation 2003; 22: 2045-2050.

[7] Budhram GR, Mader TJ, Lutfy L, Murman D, Almulhim A. Left ventricular thrombus development during ventricular fibrillation and resolution during resuscitation in a swine model of sudden cardiac arrest. Resuscitation 2014; 85: 689-693.

[8] Lian WS, Lin H, Cheng WT, Kikuchi T, Cheng CF. Granulocyte-CSF induced inflammation-associated cardiac thrombosis in iron loading mouse heart and can be attenuated by statin therapy. J Biomed Sci 2011; 15: 18-26.

[9] Günther F, Heidt T, Kramer M, Khanicheh E, Klibanov AL, Geibel-Zehender A, Ferrante EA, Hilgendorf I, Wolf D, Zirlik A, Reinöhl J, Bode C, Peter K, Kaufmann BA, Mühlen CVZ. Dual targeting improves capture of ultrasound microbubbles towards activated platelets but yields

no additional benefit for imaging of arterial thrombosis. Sci Rep 2017; 2: 14898.

[10] Wang X, Gkanatsas Y, Palasubramaniam J, Hohmann JD, Chen YC, Lim B, Hagemeyer CE, Peter K. Thrombus-targeted theranostic microbubbles: a new technology towards concurrent rapid ultrasound diagnosis and bleeding-free fibrinolytic treatment of thrombosis. Theranostics 2016; 20: 726-738.

[11] Maier A, Plaza-Heck P, Meixner F, Guenther F, Kaufmann BA, Kramer M, Heidt T, Zirlik A, Hilgendorf I, Reinöhl J, Stachon P, Bronsert P, Birkemeyer R, Neudorfer I, Peter K, Bode C, von Zur Mühlen C. A molecular intravascular ultrasound contrast agent allows detection of activated platelets on the surface of symptomatic human plaques. Atherosclerosis 2017; 267: 68-77.

[12] Cerşit S, Bayam E, Gündüz S, Güner A, Özkan M. Brachial embolism from mechanical mitral valve thrombosis. Blood Coagul Fibrinolysis 2018; 29: 395-398.

[13] Abdelmoneim SS, Pellikka PA, Mulvagh SL. Contrast echocardiography for assessment of left ventricular thrombi. J Ultrasound Med 2014; 33: 1337-1344.